Author/s:
Kang, Y;Qiu, R;Jian, M;Wang, P;Xia, Y;Motevalli, B;Zhao, W;Tian, Z;Liu, JZ;Wang, H;Liu, H;Zhang, X

Title:
The Role of Nanowrinkles in Mass Transport across Graphene-Based Membranes

Date:
2020-08-07

Citation:
Kang, Y., Qiu, R., Jian, M., Wang, P., Xia, Y., Motevalli, B., Zhao, W., Tian, Z., Liu, J. Z., Wang, H., Liu, H. & Zhang, X. (2020). The Role of Nanowrinkles in Mass Transport across Graphene-Based Membranes. Advanced Functional Materials, 30 (32), https://doi.org/10.1002/adfm.202003159.

Article type: Full Article

The Role of Nanowrinkles in the Mass Transport across Graphene-based Membranes

Yuan Kang, Ruosang Qiu, Meipeng Jian, Peiyao Wang, Yun Xia, Benyamin Motevalli, Wang Zhao, Zhiming Tian, Jefferson Zhe Liu, Huanting Wang, Huiyuan Liu, Xiwang Zhang**

Y. Kang, R. Qiu, Dr. M. Jian, Y. Xia, Dr. W. Zhao, Prof. H. Wang, Dr. H. Liu and Prof. X. Zhang

Department of Chemical Engineering,

Monash University,

Clayton VIC 3800, Australia

P. Wang, Prof. J. Z. Liu

Department of Mechanical Engineering,

The University of Melbourne,

Parkville VIC 3010, Australia

Dr. B. Motevalli

CSIRO Data61

Door 34 Village Street,

Docklands VIC 3008, Australia

Dr. Z. Tian

Department of Materials Engineering,

Monash University,

Clayton VIC 3800, Australia

E-mail: vincentlau1988@gmail.com

xiwang.zhang@monash.edu

Keywords: reduced graphene oxide, membranes, wrinkles, transport mechanisms

Abstract: Laminar membranes stacked by two-dimensional (2D) materials are an emerging selective unit in separating processes across disciplines for their controllable mass transport properties. In general, parallel nanochannels formed between neighboring layers, owing to their adjustable size and surface chemistry, are considered the dominant transport regulator. Besides these flat interlayer channels, wrinkled morphology has also existed in 2D membranes, but the structure and potential transporting role of such curved channel remain largely unexplored. This study demonstrates that nanowrinkles are intrinsically formed in graphene-based membranes, featuring an arc-like shape with around 2.5 nm-high center and two narrow wedge corners. By a facile "solvent-treatment" during assembly, the membranes are tuned to possess different wrinkle density. In transport tests involving water and ions, the appearance of more wrinkles yields higher water permeation yet has limited effect on ion passage. These findings suggest that nanowrinkles by themselves serve as fast transporting ways while their connection with narrow interlayer channels can form a selective network. Results here are expected to deepen our understanding of mass transport mechanisms in current laminar membranes (e.g. graphene-based) and provide strategies for designing future 2D membranes via wrinkle engineering.

1. Introduction

Engineering two-dimensional (2D) materials and assembling them into rational structures provide multiple routes to construct membranes for controllable mass transport within nanoscale.[1,2] A prevailing strategy is to exfoliate bulk materials into monolayered nanosheets, coupled with the restacking of these building blocks to form laminar membranes. In this rebuilt layered structure, spaces between adjacent nanosheets are left empty to become 2D nanochannels in both horizontal and vertical directions, which alternately combine to constitute tortuous transporting pathways.[3,4] Depending on channel geometry (size, length) and surface chemistry (charge, functionality), transport via the pathways can be regulated, allowing ultrafast permeation of target species yet blocking unwanted ones.[5] On this basis, selectivity between ions, gases and liquids is achievable to enable separations in vital environmental, resource and energy applications.[6–9]

As a major part of a typical pathway, interlayer channels are always considered the most prominent transport-controlling factor, since their size (termed as interlayer spacing) largely decides species uptake into laminar membranes. As exemplified by early studies on graphene oxide (GO) based membranes, hydrated GO membranes possess an effective interlayer spacing of around 0.9 nm, leading to the transport cutoff of large polyatomic ions (e.g. $[Fe(CN)_6]^{3-}$).[6] Moderate decrease of interlayer spacing to 0.6 nm can further impede the passage of smaller monoatomic ions (e.g. K^+ and Mg^{2+}) and, following this reasoning, ultra-narrow channels (0.1 nm) should be impermeable to even water.[10,11] However, fully reduced GO (rGO) membranes with effective channel size well below water molecular diameter have been found yielding considerable water throughput under osmotic pressure.[12] A plausible reason for this unexpected water permeation is the appearance of intrinsic defects in rGO membranes. These nanosized holes (~1 nm) formed within nanosheets, when connected each other, can guide much faster water flow via vertical cross-layer "shortcuts" instead of through much longer horizontal interlayer channels.[13] Nevertheless, more recent researches point out the low probability of this flowing mode, since the holes are easily shielded by the mutual stacking of enough nanosheets during membrane assembly.[7] Therefore, alternative channels should exist in rGO laminar membranes to obtain the decent water flux.

One possible but long overlooked channel may be created by wrinkled structures in laminar membranes. In most previous theories and simulation models, GO and rGO nanosheets were assumed to be flat and strictly parallel to each other, whereas in reality they are flexible and corrugated during assembly.[3,14,15] The presence of curved nanowrinkles amid parallel membrane layers often results in additional and wider transporting channels. This concept has then inspired the design of crumpled rGO membranes and nanostrand-channeled GO membranes for increased permeability.[16,17] Despite these efforts to externally introduce

nanowrinkles, few attention has been paid to the intrinsic ones formed in graphene-based membranes, including their structure and more importantly, their potential role in transmembrane transport.

In light of this, this study employs experimental works and molecular dynamics (MD) simulations to investigate inherent nanowrinkle structure in rGO membranes. It reveals that nanowrinkles possess an arc-like shape featuring a 2-3 nm high central part and narrower wedge corners. Moreover, by a facile solvent-treatment method, the density of these wrinkles is adjusted, leading to varied mass transport (water and ions) phenomena in rGO membranes. It is found that nanowrinkles mainly serve as fast water transport channels, while their connection with narrow interlayer channels may form a selective transporting network towards ions. These findings can offer in-depth understanding on the mass transport mechanisms in graphene-based membranes as well as strategies to develop high-performance 2D membranes via wrinkle engineering.

2. Nanowrinkle Formation and Characterization in Graphene-based Membranes

A typical 20 nm-thick GO membrane (GOM) was first vacuum-filtrated and dried on a nylon support. Scanning Electron Microscope (SEM, **Figure 1**A) showed its corrugated surface where plenty of wrinkles with width ranging from a few to hundreds of nanometers appeared. After the membrane was transferred onto a smoother glass substrate, only nanowrinkles narrower than 50 nm remained (Figure 1B), which implied that larger wrinkles could be extrinsically caused by the rough support while smaller ones were more intrinsically formed (Figure S1, Supporting Information). Atomic Force Microscope probing on silica-supported membranes revealed that these intrinsic wrinkles had a relatively uniform height of around 2-3 nm and width of tens of nanometers (Figure 1C). Nanowrinkles were also observed in GO membranes after top layers were peeled off, indicating their existence throughout the membranes (Figure S2A, Supporting Information). After GOMs were

chemically reduced to rGO membranes (rGOMs), such nanowrinkles were still found preserved, as identified by Transmission Electron Microscopy (TEM, Figure S2B, Supporting Information).

MD simulations were performed to better understand the structure of the nanowrinkles characterized above. Since rGO is physiochemically similar to pristine graphene, graphene nanosheets were used to represent rGO for a simplified simulation system. Moreover, considering that wrinkles originate from the misalignments between neighboring rGO layers during membrane assembling and drying process, we manually generated them by conducting a "squeeze-release" operation on multi-layered graphene stacks (Figure 1D and S3, Supporting Information) instead of simulating the entire membrane preparation process. In specific, a flat bottom layer was fixed to serve as a substrate while the rest of nanosheets were set free to move. Squeezing stress was applied from both sides until a certain distance ΔL (ΔL/2 for each side) was reached. Sufficient relaxing time was then allowed to release the stress, and thereafter to obtain stabilized nanowrinkles. Figure 1E-F clearly demonstrate the dependence of stabilized wrinkle morphology on ΔL. As ΔL increased, the height of the nanowrinkle keeps increasing while its width will reach the maximum value at ΔL of 2.5-3.0 nm before dropping off. Further increase of ΔL can render the simulated nanowrinkles unstable and result in missing atoms due to strong inter-atom repulsion (Figure 1F, dashed areas). Notably, both 2-layered and 6-layered stacks stabilize at an approximate height, but the maximum width of the latter is 5 times that of its 2-layered counterpart, implying that layer number can affect nanowrinkle structure, in particular width.

To study possible structural impact of layer number (N), we simulated the stabilized nanowrinkles in 2-50 layered stacks with ΔL fixed at 2.0 nm. These wrinkles have a narrow height distribution of 1.8-2.5 nm, agreeing with relatively uniform nanowrinkles observed by AFM and proving the limited effect of layer number on wrinkle height (Figure S4, Supporting Information). By contrast, wrinkle width shows a continuous rise to increasing layer number. When N is below 5, nanowrinkles have a width of only 2-3 nm and thus a small width/height ratio of around 1.0, resulting in an obvious ridge-and-valley structure. With more layers added until N reaches 10, the width increases to ~6.0 nm.

Further layer accumulation still slightly widens the wrinkle, but the width/height ratio stays in the range of 3.0-4.0 owing to enhanced bending stiffness,[18] in accordance with experimental observation. Such large horizontal dimension relative to vertical dimension thereby leads the resultant nanowrinkles to display an arch-shaped morphology featuring two wedge corners. This unique structure differs from the tube-like wrinkle model as suggested before, and may induce transporting behaviors in rGOM deviating from those in parallel interlayer channel.[17]

3. Nanowrinkle tuning in graphene-based membranes

To explore the role of nanowrinkles in mass transport, we prepared graphene-based membranes with different wrinkle density by tuning the drying process in membrane formation using different solvents. On this basis, we then investigated the water and ion permeation in these membranes. As previously reported, wrinkle formation occurs during membrane assembly, and is due primarily to the insufficient release of vacuum-induced residue stress if the trapped water between neighboring nanosheets rapidly evaporates (drying step).[14] In light of this, we mediated membrane drying process by applying ethanol or hexane on newly filtrated GOMs for wrinkle manipulation (**Figure 2**A). The as-treated membranes are denoted as GOMs-E and GOMs-H, respectively.

As shown in Figure 2B-D, compared to pristine GOMs, GOMs-E possess an increased number of nanowrinkles, whereas GOMs-H present a much smoother surface with low wrinkle density. This discrepancy can be ascribed to the diverse polarities of the applied solvents, which affects the interaction between water and nanosheets during drying process, and then alters the stacking manner of these nanosheets in dried membranes. X-ray diffraction pattern (XRD, Figure S5, Supporting Information) illustrates that fresh GOMs, showing no major characteristic peaks, are more of a disordered hydrogel where nanosheets are largely separated from each other by water. Such loosely packed structure allows polar solvents like ethanol to diffuse into the hydrogel and interact with GO nanosheets through hydrogen bonding. Since ethanol has a smaller dipole moment than water (1.69 D for ethanol, 1.85 D for water),[19] ethanol-GO hydrogen bonding is weaker than that of water-GO.

Consequently, the electronegativity of GO nanosheets reduces once the GO-bonded water molecules are gradually replaced by ethanol (GO zeta potential changed from around -40 mV in water to -10 mV in ethanol).[20,21] This process renders the nanosheets unstable and easier to precipitate without sufficient stress relaxation, thus creating more nanowrinkles. On the other hand, non-polar solvent, hexane, is immiscible with water and almost forms no hydrogen bond with GO. Water molecules are thereby confined by the hexane layer, which retards nanosheets stacking to allow longer stress releasing time for flat membranes (details in Figure S6, Supporting Information). Even after reduction treatment, the above structural difference between parent GO membranes still remains in corresponding reduced GO membranes (Figure S7, Supporting Information, denoted as rGOMs-H, rGOMs and rGOMs-E, respectively).

The as-prepared membranes were further characterized by XRD, Raman spectroscopy, and X-ray photoelectron spectroscopy (XPS) to study whether solvent treatment caused extra alterations on membrane geometry and surface chemistry. XRD spectra (Figure S8, Supporting Information) reveals that GOMs and rGOMs show a sharp 2θ peak at around 10° and 24.0°, respectively, implying well sustained layered structure after solvent addition and membrane reduction. It is, however, noted that the characteristic peak of GOMs-E slightly shifts to 9.8° compared to that of GOMs at 10.1° and GOMs-H at 10.3°, indicative of overall wider interlayer channels. This phenomenon is reasonable considering that ethanol-treated membranes contain more wrinkled areas. Such difference is also supported by Raman characterization (Figure S9, Supporting Information). GOMs-E/rGOMs-E have the largest I_D/I_G value, followed by their counterparts GOMs/rGOMs and GOMs-H/rGOMs-H, which is reportedly due to increased disorder degree when more nanowrinkles are introduced.[22] XPS characterization shows that all pristine GO membranes have highly similar C 1s region comprising four well resolved binding energy configurations, identified as 284.7, 285.3, 286.7, 287.8 eV for sp^2, sp^3 carbon, C-O (epoxy/hydroxyl) and C=O (carbonyl), respectively (Figure S10, Supporting Information). Similarly, only minor differences are observable for the two main peaks of reduced GO membranes, namely 284.5 eV for sp^2 carbon and 285.4 eV for sp^3 carbon. These characterization

results confirm that the solvent treatment indeed presents a viable wrinkle-tuning method for graphene-based membranes without interfering with overall geometrical and chemical properties.

4. The role of Nanowrinkles in Transmembrane Mass Transport

The transporting properties of nanowrinkles were subsequently evaluated by a forward osmosis (FO) process through rGO membranes (**Figure 3**A). In the FO test, water was driven to travel across membranes from a feed solution (deionized water) to a draw solution (1 M NaCl) by osmotic pressure (concentration gradient) rather than external hydraulic force. Therefore, membrane geometric deformations imposed by external forces are negligible. Moreover, since most oxygen-containing functional groups have been removed from rGO membranes, the effect of surface charges and ion-channel interactions on mass transport is minimized. A commercial HTI FO membrane was also tested under the same condition for comparison.

As summarized in Figure 3B, water permeation through rGO membranes is positively correlated with membrane wrinkle density. While the water flux of original rGOMs reaches 25 L m^{-2} h^{-1}, this value is decreased by 70% for rGOMs-H, but doubled for rGOMs-E, being 6 times higher than that of the commercial one. Such trend implies that the emergence of nanowrinkles amid compact rGO networks is likely to promote water throughput. To verify it, we employed MD to simulate water flow through nanowrinkles in the FO process. In our model, a typical nanowrinkle (**Figure 4**A, height of 2.2 nm and width/height ratio of 3.9) was connected with two reservoirs containing water and NaCl solution, respectively, to replicate the above experimental condition. A carbon nanotube (CNT) with approximate size (diameter 3.7 nm, Figure 4B) was also simulated and compared since it is commonly viewed as a fast transport channel. Figure 4C shows that the number of water molecules travelling across the nanowrinkle is close to that across the CNT over the same time. As a widely observed phenomenon, ultrafast flow achieved in CNT is believed to result from low-friction water slip over its hydrophobic inner wall.[23] Considering the highly similar physicochemical properties of CNT and graphene (CNT is viewed as wrapped graphene), this slip theory can be extended to explain the

enhanced flow in graphene-based nanowrinkles. For a quantitative analysis, the flow enhancement caused by the slip effect is estimated here by Equation (1):[24]

$$\varepsilon = \frac{Q_S}{Q_N} = \left(1 + \frac{6L_S}{\delta}\right) \quad (1)$$

where ε is flow enhancement factor, Q_S is slip flow rate, Q_N is non-slip flow rate, L_S is slip length and δ is channel size. The average diameter of nanowrinkles is approximated as 2 nm, and the slip length in similar CNT channels is estimated no less than 100 nm according to previously reported data.[25] The calculated flow enhancement factor should be more than 300, which suggests that a much facilitated water transport is theoretically achievable in nanowrinkles.

Unlike water, ions exhibit transmembrane passage irrespective of wrinkle density. The NaCl flux through three different membranes falls in a narrow range from 1.2 to 1.5 g m^{-2} h^{-1} (Figure 3B, inset), all well below that of the commercial HTI membrane (8.0 g m^{-2}). This low value is somewhat surprising considering the size of nanowrinkles (~2 nm), which is too large to block hydrated salt ions (Na^+ and Cl^-, ~0.7 nm) by size sieving effect. Corresponding simulation also confirms that though these ions are denied access to narrower corners, they can stream into nanowrinkles easily via the wider central area, showing only modest selectivity (Figure S11, Supporting Information). To explain the possible mechanisms underlying the above transporting phenomena, we recall the wrinkle distribution in our rGO membranes. It can be seen from Figure 2 that the majority of nanowrinkles are bridged by interlayer channels, rather than immediately interconnected with each other, even in rGOMs-E with highest wrinkle density. Therefore, water and ions are supposed to go through nanowrinkles and narrow interlayer channels alternately when traveling across a membrane (Figure S12, Supporting Information). While wrinkles provide general fast transport tracks, these tight interlayer channels act as a gate that restricts ion flow but allows water flow from one wrinkle to another. Although the interlayer spacing of our rGO membranes measured by XRD translates into a size even smaller than water molecules, it is noteworthy that this value is averaged, and part of the interlayer channels should be large enough to be water permeable.[12] Undoubtedly, further elaborate

works are still needed to fully elucidate the roles of the inner rGO membrane structure in mass transport. However, we can conclude that nanowrinkles enable ultrafast mass transport, while a network comprising them and narrower interlayer channels presumably renders the membrane selective.

5. Conclusion

In conclusion, our experimental and simulation results reveal that intrinsic nanowrinkles can be stably formed and tuned in graphene-based membranes. Due to their unique arc-shaped structure and hydrophobic inner surface, they serve as fast tracks for water to enhance its permeability through the membranes. Though these nanowrinkles are non-selective to ions by themselves, they may still connect with narrow interlayer channels to constitute selective transporting networks in rGO membranes. Moreover, since nanowrinkles broadly exist within flexible 2D nanosheets, they are expected to show critical transport-controlling effects in other layered membranes as well. These insights will thus not only help understand the mass transport in existent membranes, but also inspire the design of new perm-selective 2D membranes via wrinkle engineering.

6. Experimental Section

Fabrication of GO membranes: Graphene oxide aqueous dispersion was prepared from natural graphite powder using the modified Hummers method as described in our previous study.[12] In order to fabricate GO membranes with different thicknesses, a series of GO dispersion with concentrations ranging from 0.2 to 10 μg ml^{-1} could be prepared by diluting the GO stock with DI water. The diluted GO solution (50 ml) was then filtrated on a nylon filter (47 mm, 0.45 μm Sterlitech) by vacuum filtration, which took approximately 11 mins. After filtration, the supported hydrogel GO membrane was dried at ambient conditions for 24h, which was denoted as GOMs. GOMs-E and GOMs-H were prepared by carefully adding ethanol and hexane, respectively, on the top surface of the as-filtrated GO membranes. The membranes were then transferred to a 90 mm glass petri dish, followed by further adding solvents until the membrane was fully immersed. After being kept in the solvents for

24h, the membranes were dried at ambient conditions for at least another 24h for residual solvent evaporation.

Fabrication of rGO membranes: The dried nylon supported GO membranes (GOMs-H, GOMs and GOMs-E) were placed above a 250 ml beaker containing 0.5 ml HI solution with the nylon filter side facing down. The HI solution was then heated to 80 °C . The treatment was stopped when the color of the membranes changed from light yellow to dark gray. The resultant membranes (rGOMs-H, rGOMs and rGOMs-E) were then kept in oven at 80 °C for 3h to remove HI residue. Freestanding rGO membranes were prepared by the same procedure, but using AAO filters as the support and more concentrated GO dispersion (10 μg ml^{-1}) as the filtrate. The obtained rGO membranes could easily detach from the AAO support after immersion in water, forming freestanding rGO membrane.

FO tests for freestanding rGO membranes: A laboratory-scale FO system with an effective membrane area of 0.2 cm^2 (0.25 cm in diameter) was used to determine water and reverse salt flux across rGO membranes. The feed solution was DI water and the draw solution was 1M NaCl aqueous solutions. The feed and draw solutions were circulated with peristaltic pumps. The feed side was equipped with a weight balance to record the weight change and a conductivity meter for recording the conductivity change. The water flux was calculated by:[27]

$$J_W = -\frac{\Delta w}{s\,t} \quad (1)$$

where Δw is the weight change of the feed solution, s is the effective membrane area and t is the running time. The reverse salt flux was calculated by: [27]

$$J_S = \frac{C_t V_t - C_0 V_0}{s\,t} \quad (2)$$

where C_0 and V_0 are initial solute concentration and initial feed volume, respectively, while C_t and V_t are solute concentration and the feed volume over a running time t. The solute concentration of feed solution was calculated from its conductivity.

Characterizations: The morphology of the GO/rGO membranes was examined by scanning electron microscopy (SEM, FEI Magellan 400 FEG) and transmission electron microscopy (TEM, FEI Tecnai G2 T20 TEM operating at 200 kV). Membrane height profile was obtained by atomic force microscopy (Bruker AFM Dimension Icon, USA). The layered structure of the membranes was examined by both X-ray diffraction patterns (XRD, Rigaku diffractometer with Cu Kα irradiation) and Raman spectroscopy (Renishaw inVia Raman Microscope, Chameleon He–Ne laser generator with λ= 532 nm), while the latter was also employed to investigate the carbon state of these graphene-based membranes. To further determine membrane chemical property, including functional groups, X-ray photoelectron spectroscopy was used (XPS, AXIS Ultra spectro, Kratos Analytical, Manchester, UK) with an Al K anode (1486.6 eV photon energy, 0.05 eV photon energy resolution, 300 W).

Molecular Dynamics Simulations: MD simulations were performed using LAMMPS package. Two processes were studied, including nanowrinkle formation in graphene-based membranes, and the permeation of water and salt through a nanowrinkle (and a CNT for comparison).

AIREBO potential was employed for wrinkle formation simulation with the scale factor at 3.0.[28] Both LJ and TORSION terms were on. Time step was set at 0.00025 fs. The whole system was in NPT-ensemble at 300 K during the simulation. Two faces of X direction were set fixed, while the periodic boundary conditions were applied to both Y and Z directions. In Y direction, which was along the wrinkle, the sizes of graphene sheets were extended after applying the periodic boundary condition. In Z direction, which was vertical to the substrate nanosheet, the simulation boundaries were set over 90 Å away from the graphene sheets for system equilibrium. Wrinkle formation simulation was conducted along the following process (Figure S3, Supporting Information): The bottom substrate layer was kept fixed and flat throughout the whole simulation, while the other sheets were free to move. To initiate a wrinkle, both sides of movable sheets in X direction were applied with forces pointed towards to the center after an upward force acting on the middle parts of the sheets. Till a certain distance ΔL (ΔL/2 from both sides) was reached, the squeezing was stopped by

setting all atoms' velocities at 0. Then a sufficient simulation time was applied to release the stress caused by the squeezing to obtain stabilized nanowrinkles.

In simulations involving water and salt permeation through nanowrinkles, the stabilized wrinkle obtained from the formation simulation was set fixed, filled with SPC/E water molecules and inserted between a water and a 1M NaCl salted reservoir (Figure S3). Lorentz-Berthelot mixing rule were used to calculate the non-bonded interaction among atoms in these simulations.[3,29] The cutoff radius of the Lennard-Jones (LJ) potential was set at 10 Å and the PPPM solver was used for the electrostatic potential. All SPC/E water molecules were employed with SHAKE algorithm and all solution molecules moved in NVT at 298 K with a time step at 1 fs. Periodic boundary condition was applied to all directions although the boundaries in X direction were far away from the reservoir to avoid interference. Same operation was conducted for a CNT as well. The simulated nanowrinkle is set to have a geometric width of 8.6 nm and height of 2.2 nm (weight/height ratio around 3.9) to replicate the real ones in 50-layered membranes, giving a cross-sectional surface area of 11.4 nm^2. Correspondingly, the CNT is defined to have a diameter of 3.7 nm, giving an approximate area of 10.7 nm^2. The number of atoms inside a nanowrinkle was collected every 5 ps for 700 times and plotted with average molecule number per $Å^3$ to calculate the transport area of molecules (Figure S11, Supporting Information).

Supporting Information

Supporting Information is available from the Wiley Online Library or from the author.

Acknowledgements

Primary support for this project was provided by the Australian Research Council under IH170100009. X.Z. thanks the Australian Research Council and the Monash University for his ARF and Larkins Fellowships. Y.K. and R.Q. would like to thank Monash University for their scholarships. Y.K. and R.Q. contributed equally to this work. The authors also thank Dr. Yinlong Zhu and Dr. Xiangkang Zeng for their help with characterization works.

Received: ((will be filled in by the editorial staff))
Revised: ((will be filled in by the editorial staff))
Published online: ((will be filled in by the editorial staff))

References

[1] B. Mi, *Science.* **2019**, *364*, 1033.

[2] G. Liu, W. Jin, N. Xu, *Angew. Chemie - Int. Ed.* **2016**, *55*, 13384.

[3] R. R. Nair, H. A. Wu, P. N. Jayaram, I. V. Grigorieva, A. K. Geim, *Science.* **2012**, *335*, 442.

[4] B. A. R. Koltonow, J. Huang, *Science.* **2016**, *351*, 1395.

[5] Y. Kang, Y. Xia, H. Wang, X. Zhang, *Adv. Funct. Mater.* **2019**, 1902014.

[6] R. K. Joshi, P. Carbone, F. C. Wang, V. G. Kravets, Y. Su, I. V. Grigorieva, H. A. Wu, A. K. Geim, R. R. Nair, *Science.* **2014**, *343*, 752.

[7] Q. Yang, Y. Su, C. Chi, C. T. Cherian, K. Huang, V. G. Kravets, F. C. Wang, J. C. Zhang, A. Pratt, A. N. Grigorenko, F. Guinea, A. K. Geim, R. R. Nair, *Nat. Mater.* **2017**, *16*, 1198.

[8] J. Shen, G. Liu, Y. Ji, Q. Liu, L. Cheng, K. Guan, M. Zhang, G. Liu, J. Xiong, J. Yang, W. Jin, *Adv.*

Funct. Mater. **2018**, *28*, 1801511.

[9] G. Liu, J. Shen, Y. Ji, Q. Liu, G. Liu, J. Yang, W. Jin, *J. Mater. Chem. A* **2019**, *7*, 12095.

[10] W. Li, W. Wu, Z. Li, *ACS Nano* **2018**, *12*, 9309.

[11] Y. Su, V. G. Kravets, S. L. Wong, J. Waters, A. K. Geim, R. R. Nair, *Nat. Commun.* **2014**, *5*, 1.

[12] H. Liu, H. Wang, X. Zhang, *Adv. Mater.* **2015**, *27*, 249.

[13] Y. Han, Z. Xu, C. Gao, *Adv. Funct. Mater.* **2013**, *23*, 3693.

[14] X. Shen, X. Lin, N. Yousefi, J. Jia, J. K. Kim, *Carbon.* **2014**, *66*, 84.

[15] F. Zheng, Q. H. Thi, L. W. Wong, Q. Deng, T. H. Ly, J. Zhao, *ACS Nano* **2020**.

[16] D. Li, L. Qiu, G. P. Simon, Y. Wang, W. Yang, X. Zhang, *Chem. Commun.* **2011**, *47*, 5810.

[17] H. Huang, Z. Song, N. Wei, L. Shi, Y. Mao, Y. Ying, L. Sun, Z. Xu, X. Peng, *Nat. Commun.* **2013**, *4*, 1.

[18] X. Chen, C. Yi, C. Ke, *Appl. Phys. Lett.* **2015**, *106*, 2.

[19] D. Konios, M. M. Stylianakis, E. Stratakis, E. Kymakis, *J. Colloid Interface Sci.* **2014**, *430*, 108.

[20] D. Li, M. B. Müller, S. Gilje, R. B. Kaner, G. G. Wallace, *Nat. Nanotechnol.* **2008**, *3*, 101.

[21] D. H. Kim, Y. S. Yun, H. J. Jin, *Curr. Appl. Phys.* **2012**, *12*, 637.

[22] Y. Sun, J. Tang, K. Zhang, J. Yuan, J. Li, D. M. Zhu, K. Ozawa, L. C. Qin, *Nanoscale* **2017**, *9*, 2585.

[23] B. J. H. Mainak Majumder, Nitin Chopra, Rodney Andrew, *Nature* **2005**, *438*, 44.

[24] N. Wei, X. Peng, Z. Xu, *ACS Appl. Mater. Interfaces* **2014**, *6*, 5877.

[25] J. K. Holt, H. G. Park, Y. Wang, M. Stadermann, A. B. Artyukhin, C. P. Grigoropoulos, A. Noy, O.

Bakajin, *Science.* **2006**, *312*, 1034.

[26] H. Liu, Z. Xing, J. Zhang, J. H. Pan, H. Wang, X. Zhang, *Adv. Mater. Interfaces* **2016**, *3*.

[27] X. Song, Z. Liu, D. D. Sun, *Adv. Mater.* **2011**, *23*, 3256.

[28] S. J. Stuart, A. B. Tutein, J. A. Harrison, *J. Chem. Phys.* **2000**, *112*, 6472.

[29] S. Chowdhuri, A. Chandra, *J. Chem. Phys.* **2001**, *115*, 3732.

Figures

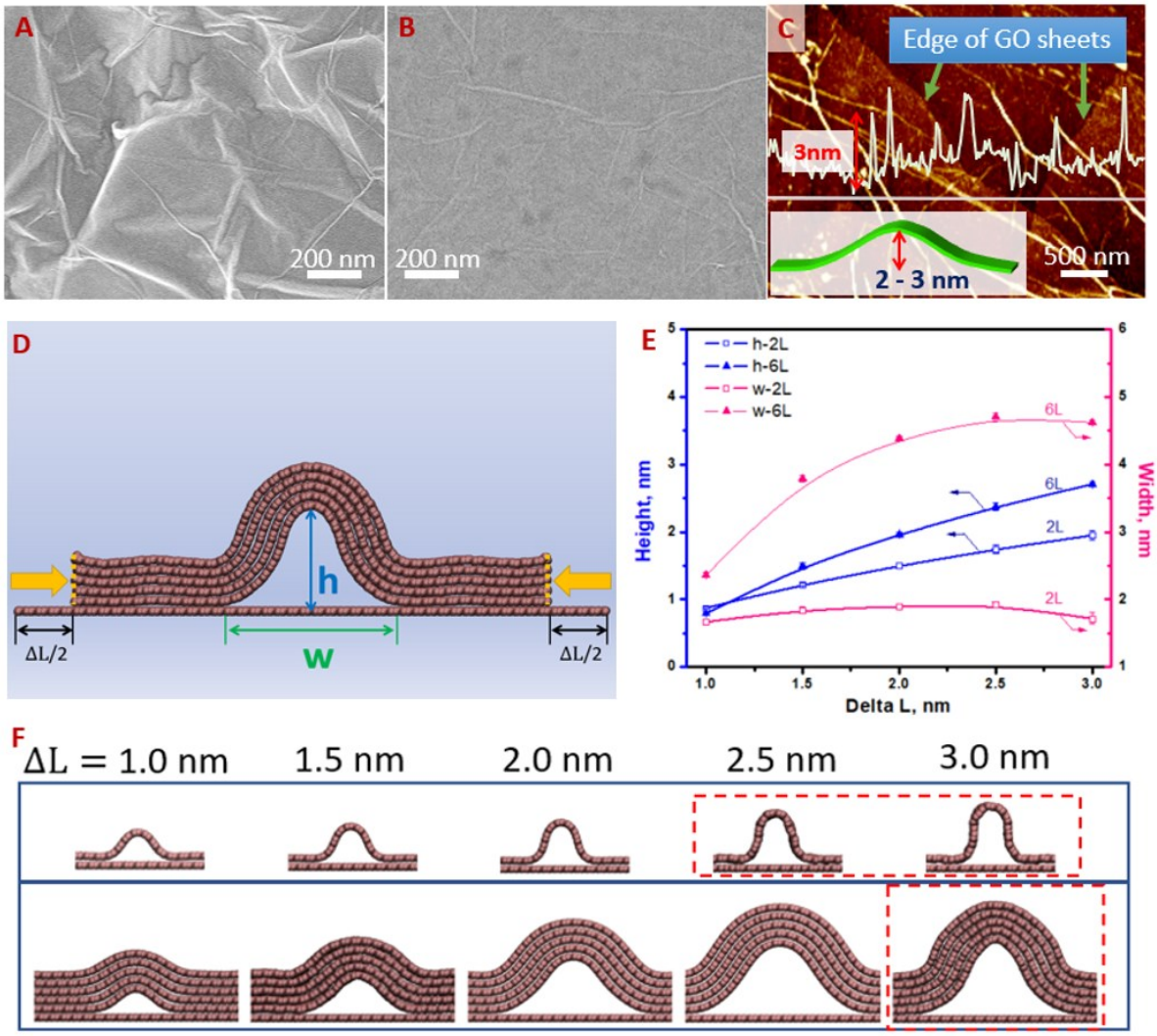

Figure 1. Nanowrinkle formation in graphene-based membranes. (A-B) SEM images of GOMs on (A) a nylon filter and (B) a glass substrate. (C) AFM height profile of a silica-supported GOM. (D-F) Simulations of nanowrinkle formation in rGOMs. (D) "Squeeze-release" simulation model for wrinkle generation. Squeeze was applied on graphene stacks from both sides and released until a certain ΔL was reached. (E) Height and width change of nanowrinkles in 2-layered and 6-layered stacks as a function of ΔL, and (F) corresponding simulation snapshots that reflect the change. Red dashed areas indicate unstable regions during the simulation.

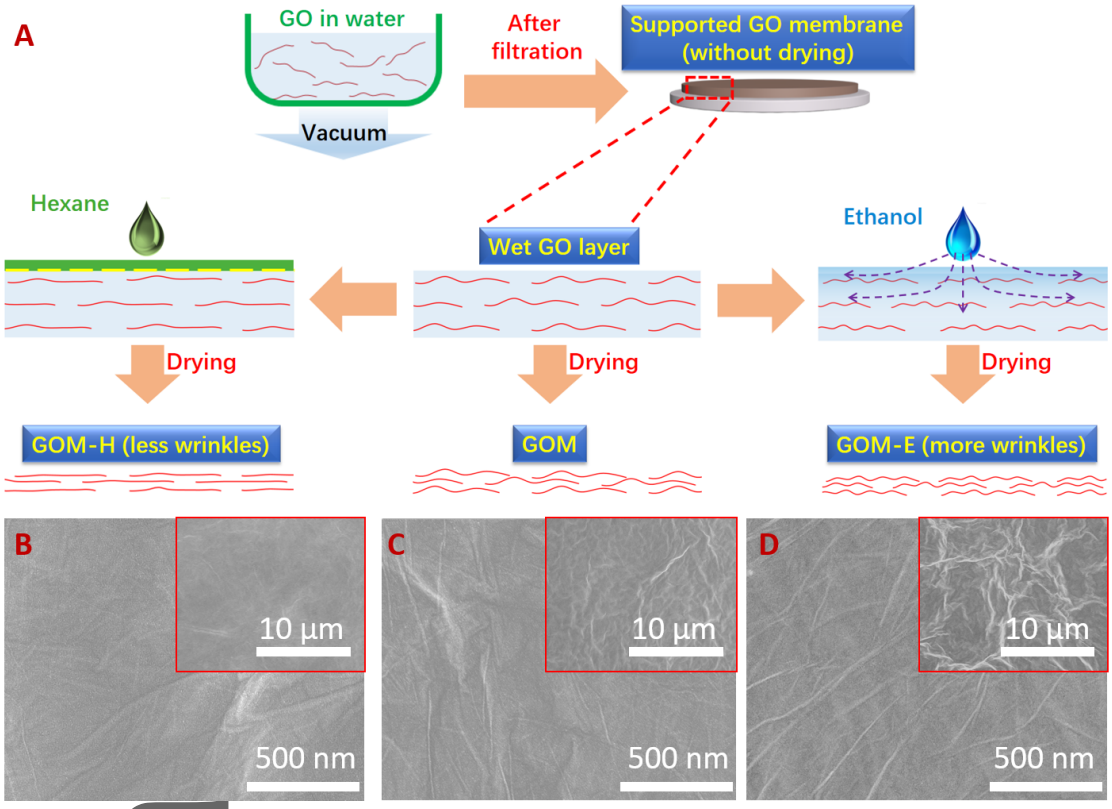

Figure 2. Wrinkle engineering in GO membranes. (A) Schematic of wrinkle engineering in GO membranes. Hydrogel-like GO membranes were prepared by vacuum filtrating GO dispersion, immediately followed by hexane or ethanol addition for decreased or increased wrinkle density, respectively. (B-D) SEM images of freestanding (B) GOMs-H, (C) GOMs and (D) GOMs-E.

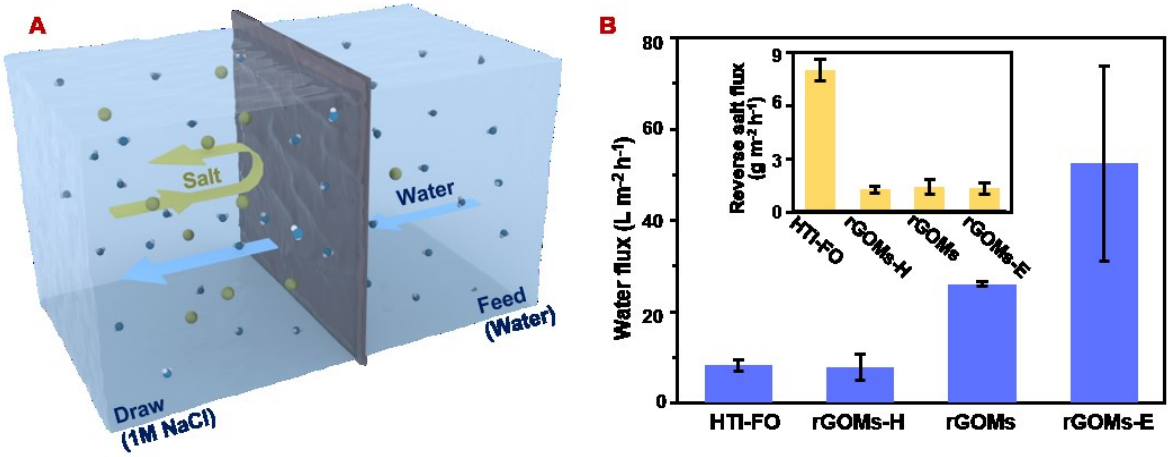

Figure 3. Mass transport through rGOMs. (a) Schematic diagram of a FO process. (b) FO performance (water and reverse salt flux) of freestanding rGO membranes with adjusted wrinkle densities, and of a commercial FO membrane from HTI for comparision purpose.

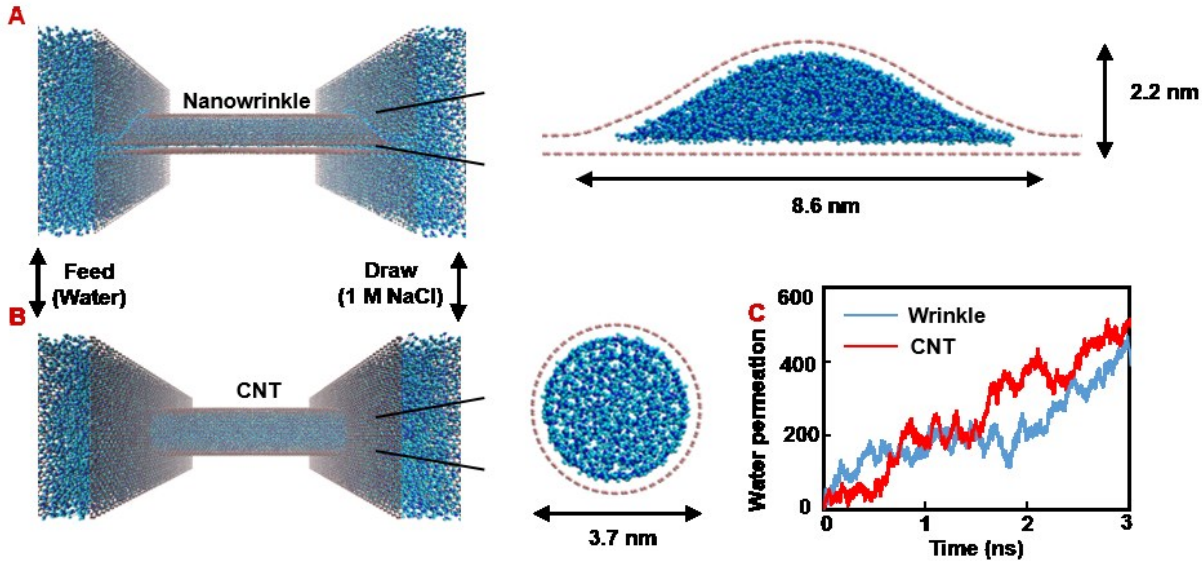

Figure 4. Simulations of fast water transport through nanowrinkles. Simulation model for water transport from a water reservoir (feed) to a saline reservoir (draw) through (A) a nanowrinkle and (B) a CNT. The cross-sectional configurations show that both channels possess similar size. (C) Comparison of water permeation through the wrinkle and the CNT, defined by the number of water molecules transported to the draw reservoir over 3 ns.

Two-dimensional (2D) layered membranes are a multidisciplinary selective unit for possessing parallel interlayer channels to control mass transport. Besides these flat channels, wrinkled structure can also appear to affect the transport in the membranes. The formation and tuning of nanowrinkles are thus studied in graphene-based membranes, which offers a way to understand the role of nanowrinkles to regulate mass transport in 2D membranes.

Keyword: Nanostructure membranes

Yuan Kang, Ruosang Qiu, Meipeng Jian, Peiyao Wang, Yun Xia, Benyamin Motevalli, Wang Zhao, Zhiming Tian, Jefferson Zhe Liu, Huanting Wang, Huiyuan Liu*, Xiwang Zhang*

Title: The Role of Nanowrinkles in the Mass Transport across Graphene-based Membranes

ToC figure ((Please choose one size: 55 mm broad × 50 mm high **or** 110 mm broad × 20 mm high. Please do not use any other dimensions))